

CALCULATION OF CLOUD MOTION WIND WITH GMS-5 IMAGES IN CHINA

Xu Jianmin Zhang Qisong

**Satellite Meteorological Center
Beijing 100081, China**

ABSTRACT

With GMS-5 images, cloud motion wind was calculated. For more accurate result and less calculation amount, the algorithm includes three major essentials:

Geometric Formula

In calculation of wind direction and speed, spiracle triangle formulas under great circle principle were adopted.

Height Assignment

For clouds above peak of water vapor channel weighting function, IR and WV channels were both used to identify heights, and a simple arithmetic resolution avoids the need of upwelling radiance integration; for clouds below peak of weighting function, only IR channel was used to identify heights.

Calculation Procedure

Rather than full correlation coefficient matrix being calculated, a calculation procedure was adopted. With this procedure, only about 1/8 points on the matrix need to be calculated for the maximum to be picked out. This procedure was tested by big amount of data and was improved effective. With this procedure the cloud motion wind program was run at a PC 486. A full disk 2.5 deg. grid wind field calculation with three images took about 40 minutes.

1. Introduction

Since the automated technique based on the use of cross correlation was introduced by Leese et al. (1971) for determine cloud motion wind from geostationary meteorological satellite images, the cross correlation technique has been adopted by all major operational satellite data processing centers (Merrill et al, 1991; MSC, 1989; Schmetz, 1993). Improvements to the technique include: height assignment by using water vapor channel (Schejwach, 1982), height assignment by using CO₂ absorbent channel (Menzel et al, 1983), tracer image filtering (Hoffman, 1990) and automatic quality control (Hyden, 1995). Satellite Meteorological Center of China tested to calculate cloud motion winds with GMS-5 data from JMA.

This paper introduces three major essentials in our wind calculation technique which are different from the other techniques or are the ones not yet been described by the published

papers. Section 2 of this paper describes the formula used for wind direction and speed calculation on spheroidal earth. Section 3 refers to our height assignment procedure. For semi-transparent cirrus clouds, both IR and WV channels are used to assign cloud height, and a simple arithmetic resolution avoids the need of upwelling radiance integration. Section 4 illustrates a quick search procedure which catches maximum of the correlation coefficient matrix with about 1/8-1/10 amount of calculation.

2. Wind Direction and Speed on Spheroidal Earth

Fig 1 shows a tracer moving from A(φ_A, λ_A) to B(φ_B, λ_B). φ_A and φ_B are latitudes of A and B respectively; λ_A, λ_B longitudes; $\Delta\lambda$ the longitude difference between B and A; r earth radius; N north pole. Note that all three arcs of a spherical triangle are on the great circles of the sphere. That means $\gamma = \angle AOB = AB$, $\angle N = \lambda_B - \lambda_A = \Delta\lambda$. Wind direction should be angle A of the spherical triangle NAB. Wind speed should be arc length AB of the spherical triangle NAB.

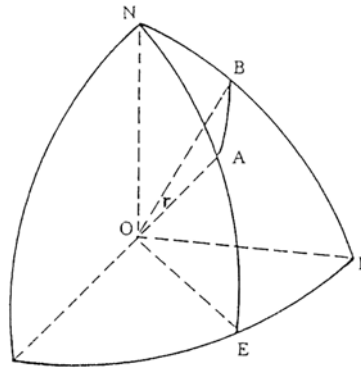


Fig 1. Tracer movement on sphere earth

In case of spherical earth, based on law of cosines for spherical triangle NAB,

$$\begin{aligned} \cos \gamma &= \cos(90^\circ - \varphi_A) \cos(90^\circ - \varphi_B) + \sin(90^\circ - \varphi_A) \sin(90^\circ - \varphi_B) \\ &= \sin \varphi_A \sin \varphi_B + \cos \varphi_A \cos \varphi_B \cos \Delta\lambda \end{aligned} \quad (1)$$

Thus arc length $AB = \gamma r$, Wind speed

$$fff = \gamma r / \Delta t \quad (2)$$

In formula (2), Δt is time interval from the time the radiometer to scan point A at the first image, to the time the radiometer to scan point B at the second image. Further, based on law of cosines for spherical triangle ABN,

$$\cos(90^\circ - \varphi_A) = \cos \gamma \cos(90^\circ - \varphi_B) + \sin \gamma \sin(90^\circ - \varphi_B) \cos A$$

Thus

$$A = \cos^{-1} [(\sin \varphi_B - \cos \gamma \sin \varphi_A) / (\sin \gamma \cos \varphi_B)] \quad (3)$$

In case of $\lambda_B > \lambda_A$, Wind direction

$$DD = A \quad (4)$$

In case of $\lambda_B < \lambda_A$, Wind direction

$$DD = 360^\circ - A \quad (5)$$

Formulas (1) - (5) are used to calculate wind direction and speed on spherical earth. For spheroidal earth, the earth radius is not a constant. It is a function of latitude:

$$r = r_p \sqrt{(1 + tg^2 \varphi) / (1 + tg^2 \varphi - \varepsilon^2)} \quad (6)$$

In formula (6), r_p is earth radius at the pole, ε is the eccentricity of the earth.

3. Height Assignment

Height assignment with IR and WV channels was firstly introduced by Szejwach (1982). He discovered the linear relationship between IR and WV radiance viewing different cloud amounts. This relationship combined with radiation transfer integration at variety of opaque cloud condition gives height estimation for opaque cloud.

The height assignment procedure we used avoids to make radiation transfer integration. Fig 2 and Fig 3 are scheme diagrams to illustrate the physical bases of our procedure. Fig 2 shows origins of IR and WV channel radiance at different cloud conditions. In Fig 2, the curves labeled with WV and IR at the most left part of the figure show the priority function of the two channels with height. IR and WV represent infrared and water vapor respectively.

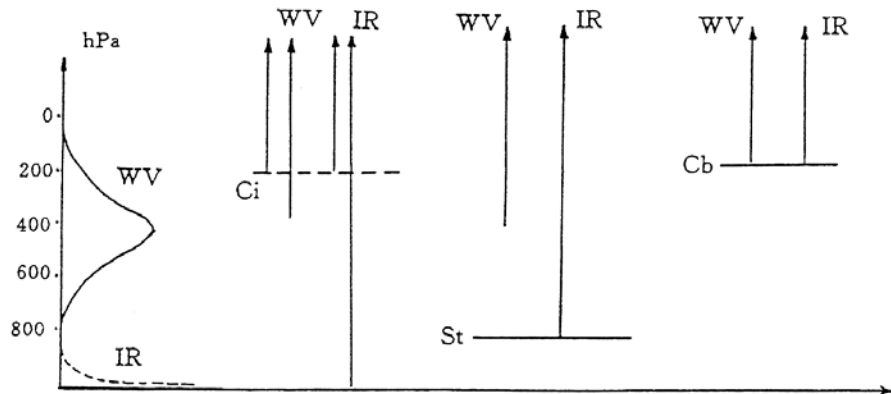


Fig 2 Origins of IR and WV channel radiance at different cloud conditions

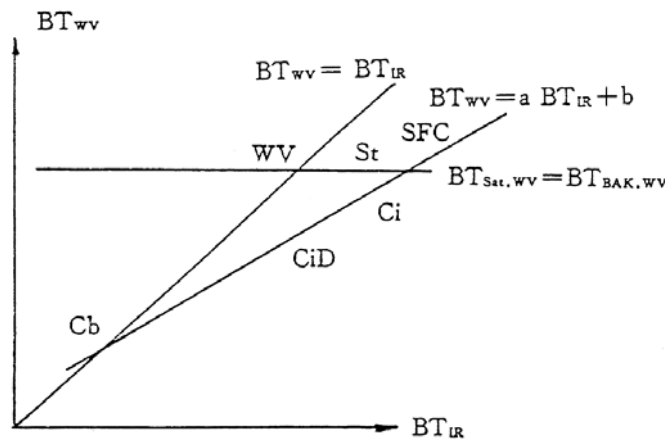


Fig 3 Scatter diagram of IR and WV brightness temperature at different cloud conditions.

3.1 Semi-transmittance Cirrus Cloud

In case of Semi-transmittance cirrus cloud, parts of the radiance origin from the background under the cloud. For IR channel the background radiance is from the surface, for WV channel it is from the upper troposphere. This can be expressed as

$$R_{SAT,WV} = (1 - NE_{WV})R_{RKG,WV} + NE_{WV}R_{CLOUD,WV} \quad (7)$$

$$R_{SAT,IR} = (1 - NE_{IR})R_{BKG,IR} + NE_{CLOUD,IR} \quad (8)$$

In formulas (7) and (8), R is radiance, N cloud amount, E cloud emissivity, SAT value received by the satellite, BKG originated from background, CLOUD originated from cloud. Suppose $NE_{WV} = NE_{IR} = NE$, combines (7) and (8), we get,

$$R_{SAT,WV} = aR_{SAT,IR} + b \quad (9)$$

$$a = \frac{R_{CLOUD,WV} - R_{BKG,WV}}{R_{CLOUD,IR} - R_{BKG,IR}}$$

$$b = \frac{R_{CLOUD,IR} R_{BKG,WV} - R_{BKG,IR} R_{BKG,WV} - R_{CLOUD,WV} R_{BKG,IR} + R_{BKG,IR} R_{BKG,WV}}{R_{CLOUD,IR} - R_{BKG,IR}}$$

The above linear relationship between radiance of the two channels was indicated by Schejwach (1982). In practice, as an approximation, we use brightness temperature to replace radiance in (9), that is

$$BT_{SAT,WV} = a BT_{SAT,IR} + b \quad (10)$$

$$a = \frac{BT_{CLOUD,WV} - BT_{BKG,WV}}{BT_{CLOUD,IR} - BT_{BKG,IR}}$$

$$b = \frac{BT_{cloud,IR} BT_{BKG,WV} - BT_{BKG,IR} BT_{BKG,WV} - BT_{cloud,WV} BT_{BKG,IR} + BT_{BKG,IR} BT_{BKG,WV}}{BT_{cloud,IR} - BT_{BKG,IR}}$$

Due to linear relationship between brightness temperature of the two channels expressed by (10), brightness temperature scatter diagrams do have linear characteristics as shown in scheme diagram Fig 3. Suppose there is no water vapor absorption above the cloud top, for opaque cloud, we have

$$BT_{SAT,WV} = BT_{SAT,IR} \quad (11)$$

Combine (10) and (11), we can easily get $BT_{SAT,IR}$. And $BT_{SAT,IR}$ should represent environmental temperature for the level cloud exists.

3.2 Opaque Middle or Low Level Cloud

When clouds are at the levels below water vapor channel peak priority function level, as we can see from Fig 2 that water vapor channel radiance origins from the background atmosphere. The water vapor channel brightness temperature keeps at a constant value. It does not bring us any information on the cloud. In that case, we have to assign cloud height based on IR channel only. Fortunately, most middle or low level clouds consists of water drops. Except for broken cloud with sub pixel size, these clouds are opaque. In scheme diagram Fig 3, the data points are along a line with water vapor brightness temperature as a constant. By watching many individual cases, we see that the slope a in IR-WV brightness temperature diagram is a good indicator to separate semi-transmittance cirrus cloud from opaque middle or low level clouds. The semi-transmittance cirrus cloud is along a line with slope, the opaque middle or low level cloud along a line with a constant water vapor brightness temperature.

The tracer with low level cloud can be distinguished from the tracer with cloud free area by the motion of the tracer. The tracer with cloud free area does not move.

3.3 Opaque High Level Cloud

For high level opaque clouds, we can also assume that there is no water vapor absorption above cloud level. Thus $BT_{WV} = BT_{IR}$. In the scatter diagram Fig 3, these clouds are around the cross point of formulas (10) and (11), labeled as Cb.

3.4 Height Assignment Procedure

Based on the above discussion, we get the following high assignment procedure shown in Fig 4.

4. Quick Search Procedure for Target Tracing

Target tracing with cross correlation is very computer time consuming. Fig 5 is a typical correlation coefficient matrix. In Fig 5, we calculate $33 \times 33 = 1089$ correlation coefficients just

for a maximum value 0.93 at line 21 column 14. After watching many correlation coefficient matrix, we see that most correlation coefficient fields are very smooth, e.g. the neighboring value in the matrix do not have big fluctuation. Based on this phenomena, we designed a quick search procedure.

4.1 Quick Search Procedure

The idea of quick search is to find out maximum correlation coefficient with minimum amount of calculation. As far as the maximum is found, we do not need to care coefficient values at other places.

Our quick search procedure finds out the maximum coefficient step by step. At each step, correlation coefficients are calculated at every several pixel distance. That is, we jump several pixels, then make a calculation. We name the pixel distance jumped as grid length. At the first step, the grid length should not be too big, or too small. If the grid length is too big, we may lose the real maximum. If the grid is too small, we do not save much computer time. For the following steps, we only calculate correlation coefficients around the maximums of the former steps. By each step, the grid lengths become smaller. At the last step, the grid length become one pixel, and the maximum correlation coefficient and it's position is gained.

The first step is broad search. The propose of the broad search is not to lose any possible maximum near the broad search positions. Suppose our target image window is 32 x 32 pixels. search area is 64 x 64 pixels. Thus, the effective search distance is $64 - 32 + 1 = 33$ pixels. For GMS half hourly IR image pare, this search distance insures targets moving with 50 m/s do not exceed our search boundary.

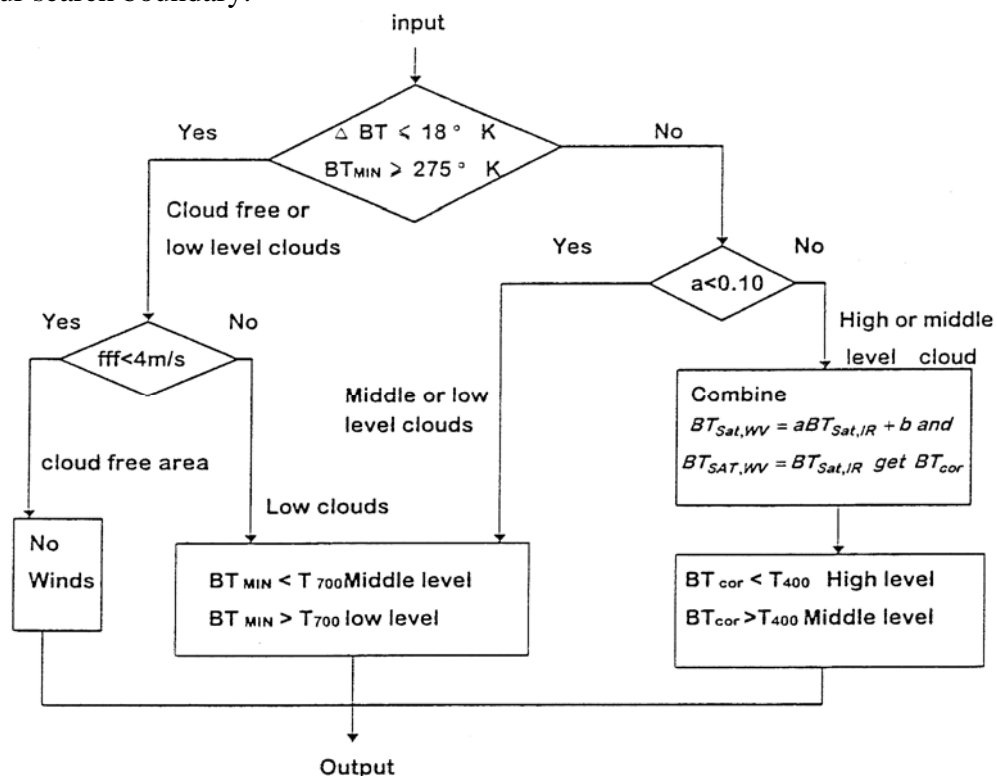


Fig 4 Height Assignment Procedure

At the first step, the grid length is designed as 8. That is, in both line and column direction, we jump 7 pixels, then calculate a correlation coefficient. By doing so, we need to calculate 25 correlation coefficients as shown in Fig 6.

For each steps from the second to the fourth, the grid length reduces to the half of the former steps. That is the grid lengths are 4, 2 and 1 pixels for steps 2, 3, 4. Search is performed only around the 6 highest coefficient values of the former steps. By the 4 steps, altogether 90-130 rather than 1089 coefficients need to be calculated. For most common cases, 118 calculation are performed. The computer time is reduced to 1/8—1/10 of the full search.

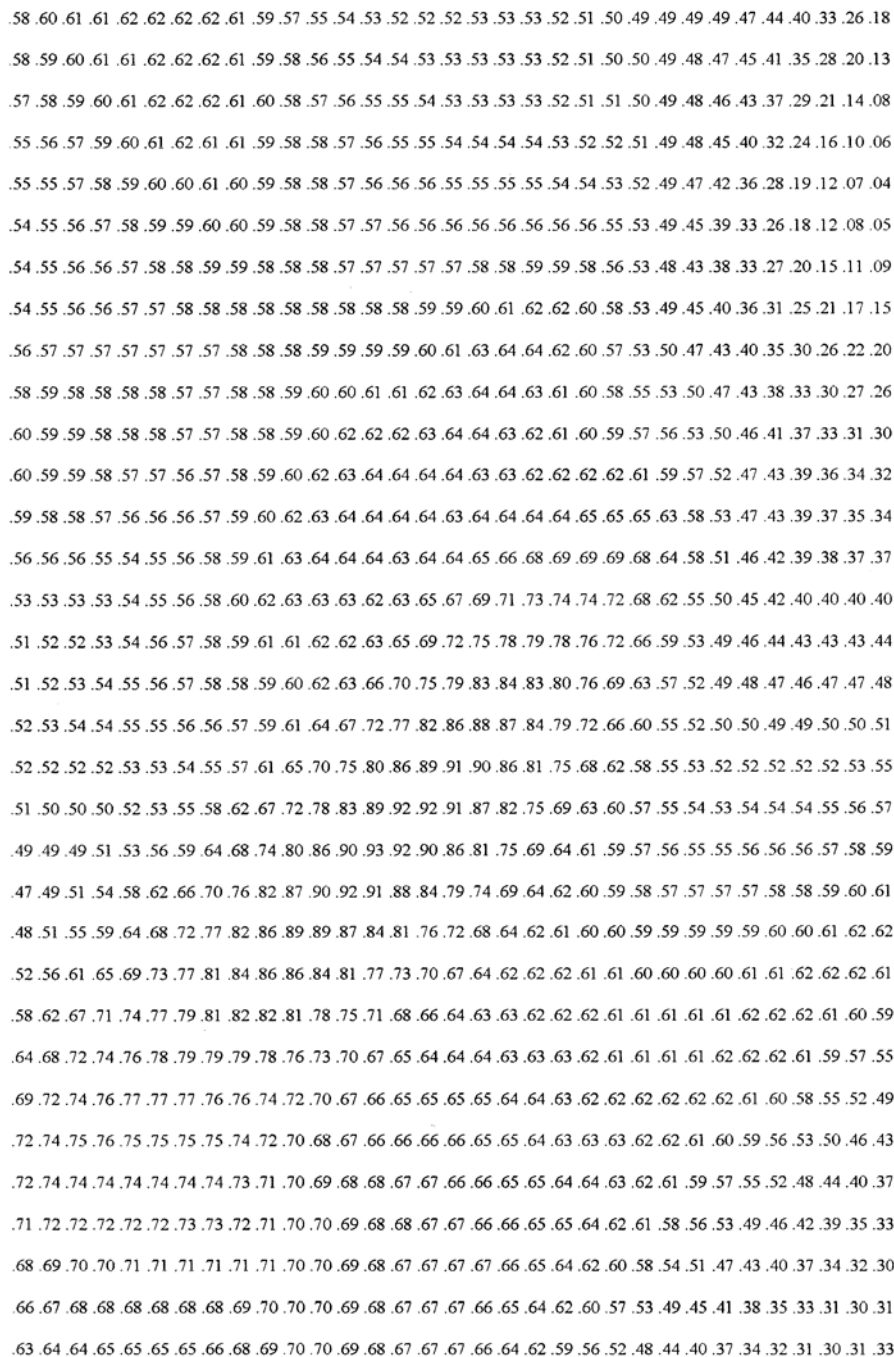


Fig 5 A typical correlation coefficient matrix

4.2 Comparison of Full Search and Quick Search

To make sure quick search procedure does not lose any maximum, an experiment calculation was made. In the experiment, 100 full search and quick search were made with the same data. The same results were gained. With a PC 486, a full search takes 57-58 seconds, while a quick search only takes 6-8 seconds.

4.3 Explanation of Quick Search Procedure

The quick search procedure works well, this is due to the common pixels in the neighboring tracer target windows. Since the existence of common pixels, the neighboring correlation coefficients are related with each other. To exam why we do not lose any possible maximum by quick search procedure. Let us simplify our problem to an one dimensional image and take an assumption that the second image is exactly a displacement of the first image.

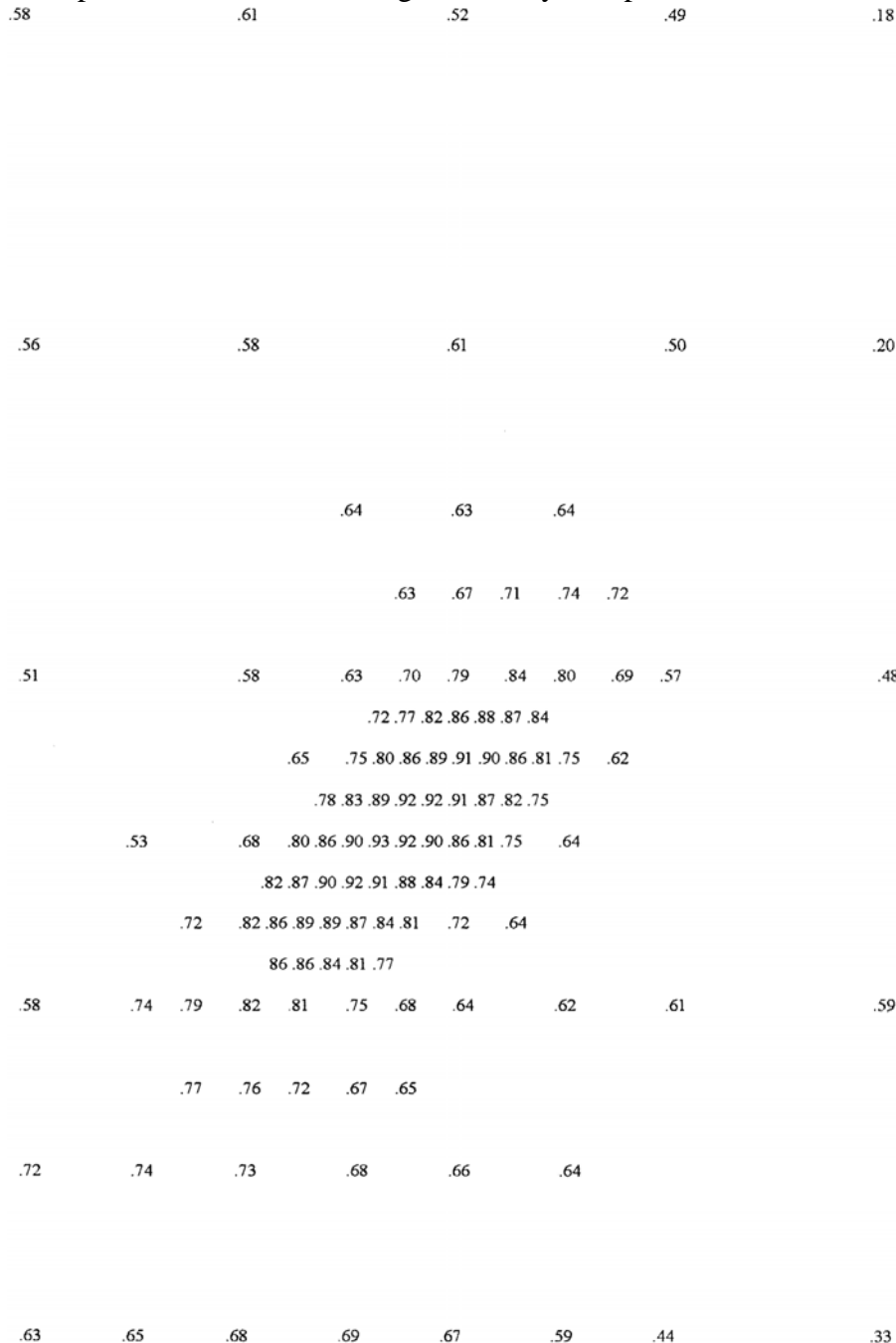


Fig 6 A typical correlation coefficient matrix calculated by quick search procedure

Suppose the target window of the first image moves and become image window “f” of the second image. At the first step of quick search procedure, we take “g” of the second image as search window, name “f” as tracer window, “g” as search window. Normally “g” is some pixels away from “f”. Because, at the first search step, we take 8 as grid length. The distance between “f” and “g” should not exceed 4 pixels. In case of 0 pixel distance, we happen to catch the tracer

at the first step. In case of 1 - 4 pixel distances, we may catch the tracer at the later steps. Remember that our image window size is 32 pixels. Now let us calculate correlation coefficients between “f” and “g”.

Tracer window “f” and search window “g” are functions expressed at space field

$$f(j) \quad (j=0,1,\dots,M-1)$$

$$g(j) \quad (j=0,1,\dots,M-1)$$

Take fourier expression of “f” and “g”, “f” and “g” can be expressed at frequency field.

$$f(j) = \sum_{K=1}^{M-1} a_{fk} \cos \frac{k\pi i}{M} + b_{fk} \sin \frac{k\pi i}{M} = \sum_{K=1}^{M-1} A_{fk} \cos \left(\frac{k\pi i}{M} - \theta_{fk} \right) \quad (13)$$

$$g(j) = \sum_{K=1}^{M-1} a_{gk} \cos \frac{k\pi i}{M} + b_{gk} \sin \frac{k\pi i}{M} = \sum_{K=1}^{M-1} A_{gk} \cos \left(\frac{k\pi i}{M} - \theta_{gk} \right)$$

In (13), $A_{fk} = \sqrt{a_{fk}^2 + b_{fk}^2}$, $A_{gk} = \sqrt{a_{gk}^2 + b_{gk}^2}$, $\theta_{fk} = \text{tg}^{-1}(b_{fk}/a_{fk})$, $\theta_{gk} = \text{tg}^{-1}(b_{gk}/a_{gk})$

Correlation coefficient R_{fg} can be expressed at frequent field as

$$R_{fg} = \sum_{i=0}^{M-1} f(i)g(i) = \sum_{K=1}^{M-1} a_{fk}a_{gk} + b_{fk}b_{gk} = \sum_{K=1}^{M-1} A_{fk}A_{gk} \cos(\theta_{fk} - \theta_{gk}) \quad (14)$$

Formula 14 shows that both amplitude and phase of “f” and “g” make contribution to the correlation between them. In case of “g” is a displacement of “f”, the correlation between them depends on the phase shifts of the specific fourier waves. Depending on the cosines of the phase differences, the specific fourier waves can make positive or negative contribution to the correlation coefficient. When an image shifts for some distance away, the larger scale characteristics of the image will have the same tendency as the original image, while smaller scale characteristics may have positive or negative tendency depending on the ratio between the shift distance and the scale of characteristics. Thus, the correlation coefficients mainly depend on larger scale characteristics of the tracer image windows. That is, when we use cross correlation method to trace tracers, what we traces are the over all pattern of the image window rather than individual clouds. This is why a 4 pixel shift of tracer does not lose any possible maximum of the correlation coefficient.

References

- Hayden C. M. and Purser R. J, 1995: Recursive Filter Objective Analysis of Meteorological Fields: Applications to NESDIS Operational Processing., J. Appl. Meteor., 34, 3-15
- Leese. J. A. and Novak. C.S, 1971:An Automated Technique for Obtaining Cloud Motion from Geosynchronous Satellite Data Using Cross Correlation, J. Appl.Meteor., 10,118-132
- McLeese. D. J. and Wilson.L.S.:1976,Cloud Top Heights from Temperature Sounding Instruments, Quart.J.R. Met. Soc., 102,781-790
- Menzel.W.P. Smith W.L. and Stewart. T.R.:1983, Improved Cloud Motion Wind Vector and Altitude Assignment Using VAS,J.Cli.Appl. Meteor.,22,377-384
- Meteorological Satellite Center: 1989,The GMS Users Guide,37-54
- Nieman.S.J. Schmetz.J.and Menzel.W.P.:1993, A Comparison of Several Techniques to Assign Heights to Cloud Tracers, J.Appl. Meteor., 32,1559-1568
- Schmetz.J. Holmlund.K. Hoffman.J.and Strauss.B.: 1993, Operational Cloud Motion Winds from Meteosat Infrared Images, J. Appl. Meteor., 32, 1206-1225
- Schejwach. G. : 1982,Determination of Semi-Transparent Cirrus Cloud Temperature from infrared Radiance Application to METEOSAT J. Appl. Meteor, 21,384-393